CHARACTERIZATION OF SILICON METAL

K. S. Chopra

Elkem Metals Company
Niagara Falls, New York

ABSTRACT

Silicon is widely used in a number of applications including, the foundry industry, steel making, aluminum alloys, ceramic components, silicones industry, and the electronic industry. These applications require different levels of silicon purity ranging from the metallurgical grade for the foundry industry to a very high purity silicon grade for the integrated circuit industry.

The characterization of silicon of all ranges of purity requires combination of tools and techniques. These include Scanning Electron Microscopy (SEM), Energy Dispersive X-ray Analysis (EDS), Auger Electron Spectroscopy (AES), Electron Microprobe, Secondary Ion Mass Spectroscopy (SIMS), and Electron Spectroscopy of Chemical Analysis (ESCA). The SEM gives high resolution and greater depth of the field image. The AES permits the analysis of surface films for all elements including the light elements, SIMS and electron microprobe yield quantitative elemental analysis. A combination of these optical and electron optics instruments and appropriate techniques have been used to characterize silicon in terms of phases present, surface chemistry, defects, inclusions, and concentration profiles of all elements, including light elements such as H, O, C, and N.

This information is helpful in obtaining an understanding of the effect of purity level and solidification rate on the grain size, precipitate size, shape, and the pattern of distribution of these silicide phases. Surface analysis techniques coupled with ion milling of the silicon surface have identified an oxide film of about 50 Å in thickness which is formed instantaneously on the surface of silicon metal. Metal silicides of Fe, Ti, Al, V, Ca, Mn, Zr, and Ni; and oxide and carbide phases within the silicon and in the grain boundaries have been fully characterized using microanalytical techniques.

Examples will show how best to utilize these sophisticated tools to understand the factors that influence the production, processing, and properties of the silicon metal.

INTRODUCTION

Silicon is one of the most widely used elements in a number of applications including, the foundry industry, steel making, aluminum alloys, ceramic components, silicones, and the electronic industry. These applications require different levels of silicon purity ranging from a metallurgical grade for the foundry industry to a very high purity silicon grade for the integrated circuit industry. Figure 1 illustrates the impurity content of various grades of silicon metal [1] available commercially. However, this is only a rough characterization of the purity of silicon. It has been repeatedly shown that material with an acceptable chemical composition need not perform satisfactorily. factors like number and shape of detrimental inclusions, macro and microstructure of the silicon metal, nature and composition of the intermetallic phases, and the presence of an oxide layer of the metal surface can play an important role for certain applications.

To produce a consistent homogeneous grade of silicon metal it is necessary to perform an optimal furnace operation, control casting, and start with selected raw material [2]. Typically, silicon metal is tapped from a submerged arc smelting furnace at 1600-1700 °C, ladle refined to meet end user industry specifications, and finally cast into cast iron chills. The tapping, refining and casting methods have a strong impact on metal quality as regards to grain structure, block segregation or homogeneity and contents of inclusions of oxides, carbides, slags and silicide phases[3].

The combination of optical microscopy along with microanalytical techniques are extremely helpful in understanding the effect of purity level and solidification rate on the grain size, grain shape and phase distribution. It also helps in the study of defect structure and other variables.

METALLOGRAPHIC ANALYSIS

The Auger Electron Spectroscopy (AES) uses an electron beam to excite a microvolume at the sample surface about 10 to 20 Å deep. It is a surface sensitive technique and ideal for applications where distribution of surface constituents must be determined. It determines all elements except hydrogen and helium. By ion sputtering one can obtain a comprehensive concentration profile.

The X-ray Energy Dispersive Analysis using a SEM provides a spectrum from a volume 2 to 5 microns deep depending upon the excitation potential used. It is an excellent technique to obtain a qualitative analysis, however, it can be used for quantitative analysis only to a limited extent.

The Electron Spectroscopy for Chemical Analysis (ESCA) uses X-ray signal to excite the sample and is thus suited for surfaces prone to damage, such as, organics, polymers, etc. This technique is better suited for precise measurement to determine binding energy, and valence state. It is also possible to do a depth profile by ion milling using the ESCA.

The Secondary Ion Mass Spectroscopy (SIMS) is a good surface analysis tool to determine trace impurity levels in a sample. It has a high sensitivity of many elements and can detect most elements, including hydrogen. A SIMS analysis requires a good known standard. SIMS can detect trace impurities in a given sample with respect to a known 'good' sample for given processing conditions.

In most situations, no single analytical technique is capable of giving definitive results. However, using a combination of techniques, wherein data from one technique supplements the data from another, can result in a conclusive analysis.

Macrostructure

The macrostructure of solid silicon metal is dependent on the cooling rate during casting. Fast cooling rates give a fine grained structure, whereas, slow cooling rates result in large grains, which grow in the cooling direction. The release of the high latent heat of silicon metal during solidification causes the solidification rate to slow down and the impurities tend to segregate in the liquid silicon metal. The ratio of concentration of a given impurity in solid silicon to its concentration in liquid silicon is low. Thus, the major impurities concentrate outside the silicon crystal and form silicides, alone or combined with other elements. These silicide phases are always located on the silicon grain boundaries between silicon grains. The composition of the silicides is given by the relative solubilities, melt composition, and cooling rate.

Figure 2 shows photographs of 5", 3", and 1 1/2" cross section of silicon castings. The castings showed segregation along its height. Samples from five positions along the height of the castings were analyzed for Fe and Al impurity levels and the results are shown in Figure 3. The top of the casting had the lowest impurity levels. The weight percent of both Fe and Al increased to a maximum at a distance equivalent of 3/4 of the casting height from the top of the casting. The variation of impurities shown in Figure 3 is determined by the cooling profiles for the given casting conditions. In general, impurities segregate to the position where the last liquid solidifies.

Microstructure

Samples with high and low level of impurities were polished for metallographic examination. Figure 4 shows representative optical microstructures of two such samples. The sample with high levels of impurities shows the existence of an intermetallic phase at grain boundaries. This intermetallic phase is minimal in the sample with low impurity levels. This suggests that the impurities within a silicon cast tend to form an intermetallic phase.

Figure 5a, at 400X, shows the typical slag inclusion present in the silicon metal. This is an exogenous inclusion entraped during the casting process. The X-ray energy dispersive analysis of the slag inclusion shown in Figure 5b identifies the presence of Si, Ca, and Al.

An infrared microscope can be used to further characterize silicon metal. A thin section of silicon metal is transparent to infrared radiation, thus, defects may be studied even though they are completely immersed in the material and do not intersect any surface. A representative optical image of silicon metal shown in Figure 6a, at 200X, depicts some inclusions within the silicon matrix. The polarized light image of the same field is shown in Figure 6b and the internal reflections indicate that the inclusion might be an oxide phase. The reflected infrared image of the same field is shown in Figure 6c, this image shows the same features as the optical image in figure 6a. However, the transmitted infrared image shown in Figure 6d resolves subsurface inclusions and defects which were not apparent in the other micrographs.

Electron Microscopy

Random samples of metallurgical grade silicon were selected to do an exhaustive study using X-ray energy dispersive analysis in SEM and electron microprobe analysis. These techniques complement each other in characterizing the phases in silicon metal.

A sample containing about 0.7 wt.% Al was examined using the optical microscope and the scanning electron microscope. The optical micrograph in Figure 7a shows an intermetallic phase in the silicon matrix. The phase appears to be a single phase in the optical microscope. However, as seen in Figure 7b, an optical image using polarized light shows that this phase is composed of a number of different phases. A backscatter SEM image of the same field is shown in Figure 7c and six phases are marked on this micrograph. The X-ray scan maps of the same field for Si, Fe, Al, and Ti are shown in Figure 7d, 7e, 7f, and 7g, respectively. X-ray spectra were obtained in the spot mode for each phase shown in Figures 7c, #1 is the silicon matrix as seen from the X-ray maps. The intermetallic phases #2 and #4 are iron silicides consisting mainly of Fe and Si with small amount of Al. These phases appear as tan or brown color in the polarized optical micrograph. On the other hand, Phase #3 contains Al, Fe, and Si in relatively equal amounts and appears as a gray phase in the optical micrograph. Phase #5 which is black in color when observed under polarized light is also composed of Fe, Si and Al, except that some of the Fe and Al are substituted by Ce. Phase #6 consists of Ti, Fe, and Si, with small amounts of Al. Thus, the different phases in the given field can be identified using the SEM and can be related to the polarized light optical micrographs. For the given sample, different fields can now be analyzed using the optical microscope having polarized light capabilities. The polarized light helps in determining the anisotropy of these silicide phases.

Figure 8a at 2000X, shows another intermetallic phase showing several phase in one particle. Figure 8b, 8c, 8d, 8e show X-ray energy dipersive spectra for phases marked in Figure 8a as #1, #2, #3, and #4, respectively. Phase #1 is a calcium silicon compound, whereas Phase #2 contains Fe, Al, Ca, and Si. The spectrum of Phase #3 indicates the major constituents is Si with small amount of Al and Mn. On the other hand, Phase #4 contains Si, Fe, and Ti as the major constituents and small amounts of Al and Mn. Figures 9 and 10, at 500X, shows the SEM image and X-ray energy dispersive spectrum of a silicon carbide inclusion and an indigenous calcium aluminate inclusion, respectively. These inclusions were identified based on the combination of the optical properties and the X-ray energy dispersive spectrum information.

A random field from the metallurgical grade silicon sample (chemical analysis shown in Table 1) was selected for extensive microanalysis using combination electron optic tools such as SEM with EDS capability, electron microprobe, Auger analysis. However, it should be noted that a good optical characterization of the sample should be done prior to doing an exhaustive electron microscopic analysis.

The optical image of the metallurgical grade silicon sample is shown in Figure 11a at 400 X, this field shows some intermetallic phases. Figures 11b and 11c show the backscatter image of the same field at 200X and 400X, respectively. X-ray image scans, using X-ray energy dispersive system for Ti, Si, Al, Fe and Ca, are shown in

Figures 11d, 11e, 11g, and 11h, respectively. The oxygen spectrum for the same field was taken by using a scanning auger system. There is an indication of oxygen in some of the intermetallic phases. Table II shows the quantitative analysis of the phases in the same field as shown in Figure 11c. An electron microprobe, capable of doing light elements such as B, C, O, and N, was used for this analysis. There was only one intermetallic phase that had oxygen slightly above the detectable limits. A spectroscan analysis was done to establish the absence of oxygen on the calcium rich (Phase #1, Figure 11) and aluminum rich (Phase #2, Figure 11) phases. The quantitative microanalysis using an electron microprobe are shown in Table II.

Auger Analysis

High purity silicon samples were fractured in air and the fractured surfaces were exposed to air for either 3 or 40 minutes. The surface chemistry of these samples were determined using Auger Electron Spectroscopy. The samples were sputtered at a rate of 30 Å/min and the concentration profiles of O, C and Si versus the sputtering time were determined. Figure 12 shows that both samples had a comparable concentration of O, C, Si on the surface. After about 1.5 minutes of sputtering, both the O and C concentrations decreased to a very low and constant level, whereas, the Si concentration increased to a constant value near 100 percent. Thus, indicating that the oxide film on the fractured surface was less than 50Å in thickness.

An Auger spectrum of a freshly fractured metallurgical grade silicon sample was obtained in the spot mode using Auger Electron Spectroscopy and is shown in Figure 13a. The spectrum identifies the presence of O, C, and Si on the freshly fractured surface. Figure 13b shows another spectrum of the sample obtained after ion milling the selected area up to a depth of 200Å. Ion milling removes the thin oxide layer on the sample and the spectrum confirms the absence of both O and C from the ion milled surface.

Further, an Auger spectrum of a random area on the surface of the sample was obtained and is shown in Figure 14a. The spectrum shows the presence of O and C on the sample surface. The 50 to 100eV range of the spectrum was expanded and is shown in Figure 14b. Two valence states of silicon can be identified from the expanded spectrum corresponding to the Si metal and the Si present as an oxide. This observation further confirms the presence of an oxide film on the surface of the silicon sample.

The Auger analysis indicate that an oxide film forms almost instantaneously on a freshly formed silicon surface. However, the oxide film is only about 50Å in depth and appears to prevent further oxidation of the metal.

Electron Spectroscopy for Chemical Analysis (ESCA)

Figure 15 shows two superimposed ESCA spectra obtained from the surface of metallurgical grade silicon sample. the dashed curve represents the spectrum of the as-received silicon surface, whereas the solid curve represents the spectrum after sputtering a 45 Å layer from the surface. The as-received sample spectrum shows a peak for both silicon and silicon dioxide. However after sputtering the silicon dioxide peak decreases considerably. Sputtering causes a shift of the silicon peak to a lower binding energy, this is quite normal.

Secondary Ion Mass Spectroscope (SIMS)

Secondary ion mass spectroscopy offers an extremely high detection sensitivity for all elements, including hydrogen. In addition, it provides isotopic and molecular information. For a typical SIMS spectrum a multitude of elements and molecules can be identified based upon the mass analysis of the secondary ions. However, the knowledge of sample history, chemistry, and a combination of techniques discussed so far can result in a positive identification of the elements and compounds present on the tested surface.

A concentration profile of C, O, N, Si, SiO, and Si_2 with respect to sputtering time was obtained for a silicon sample and is shown in Figure 16. A sputtering rate of 10Å/min was used for the determination. The spectrum shows that the O, C, and SiO decreased with sputtering time reaching a relatively constant value after about 9 minutes of sputtering, which corresponds to about 90Å depth. However, the spectrum shows that the Si concentration also decreases with sputtering time. This is because the SIMS analysis is very sensitive to the surface chemistry. On sputtering the surface chemistry changes and influences the analysis. Thus, a great deal of caution needs to be exercised when using SIMS as an analytical tool.

CONCLUSIONS

The micro and macro features of silicon metal were effectively analyzed using various characterization techniques. A complete understanding of the microstructural features was first obtained using basic optical microscopic tools. This was followed by an exhaustive analysis using electron optic tools and techniques such as Scanning Electron Microscope, Electron Microprobe, Auger, Electron Spectroscopy for Chemical Analysis (ESCA), and Secondary Ion Mass Spectroscopy (SIMS). The combination of these techniques is highly complementary and data from one can be used to supplement data from another technique.

The results from this study indicate that iron along with other impurities precipitates out as various silicide phases. The last metal to solidify is rich in these silicide phases, thus, suggesting that the area that constiutes the end of the solidification will be rich in impurities. These silicide phases of various compositions coexist at the grain boundaries. The classical theories of solidification adequately explain the rejection of impurities by the solidifying silicon metal and their segregation to the last liquid that solidifies. One thus expects more segregation of impurities during slow cooling

This study showed that indigenous oxide inclusions rarely exist in silicon metal. Since the solubility of carbon in silicon at smelting temperatures is relatively high, precipitates of silicon carbide are occasionally found within the silicon grain. It is very likely to find silicon carbide along with entraped slag, if good slag-metal separation did not take place.

The oxygen rich layer on the surface of silicon is present as an oxide and ranges from 30 to 50 Å thick. This oxide film forms within minutes of fracturing. The grain boundary phases are intermetallic silicides phases and the oxygen in these phases in below the detectable limit. A good correlation exists between the phase analysis established by different techniques. The major impurities Fe, Ca, and Al are present as silicide phases Other impurities like Ti, V,

Mn, Ni, Ce, and Cr are tied up in an iron silicide phase. This iron silicide phase appears to act as a scavenger for impurities and tramp elements.

1. A Schei, "High Purity Silicon Production", Proceedings of International Conference on Refining and Alloying of Liquid Aluminum and Ferro-Alloys, Trondheim, Norway, 1985, pp 73-89.

2. H. M. Rong, K. Forwald, A. Prestmo, G. Schussler, O. Sorli, H. A. Oye, "Quality Criteria for Silicon Used for Argano- Silicon Industy', Metall. I nt. Zeitschrift Fur Technik und Wirtschaft, Sonderdruck aus Hefr 7, 42 Jahrgang, 1988, pp.

3. G. Halvorsen and G. Shussler, "Silicon Metal Qualities for the Aluminum Industy", Internal Report,Elkem a/s, Norway.

4. E. G. Rochow, "Metallic Silicides in Silicon Alloys", The Chemistry of Silicon,Pergamon Press, 1973.

TABLE I

Chemical analysis of metallurgical grade silicon selected for characterization

Elements	weight %
Al	0.62
Ca	0.032
Cr	0.003
Cu	0.005
Fe	0.58
Mn	0.021
Ni	0.002
Ti	0.078
V	0.12
Mg	0.004
Zr	0.007
B	0.0023
C	0.053
O	0.087
N	0.003

TABLE II

Quantitative Electron Microprobe Analysis of the Phases shown in Figure 11c

Phase #	Element wt.%				
	Ca	Fe	Al	Si	O
1	5.74	34.0	25.3	34.0	nd
2	-	27.5	37.8	35.7	nd
3	-	39.5	32.3	29.7	nd
4	-	46.1	6.0	49.5	nd

nd : not determined

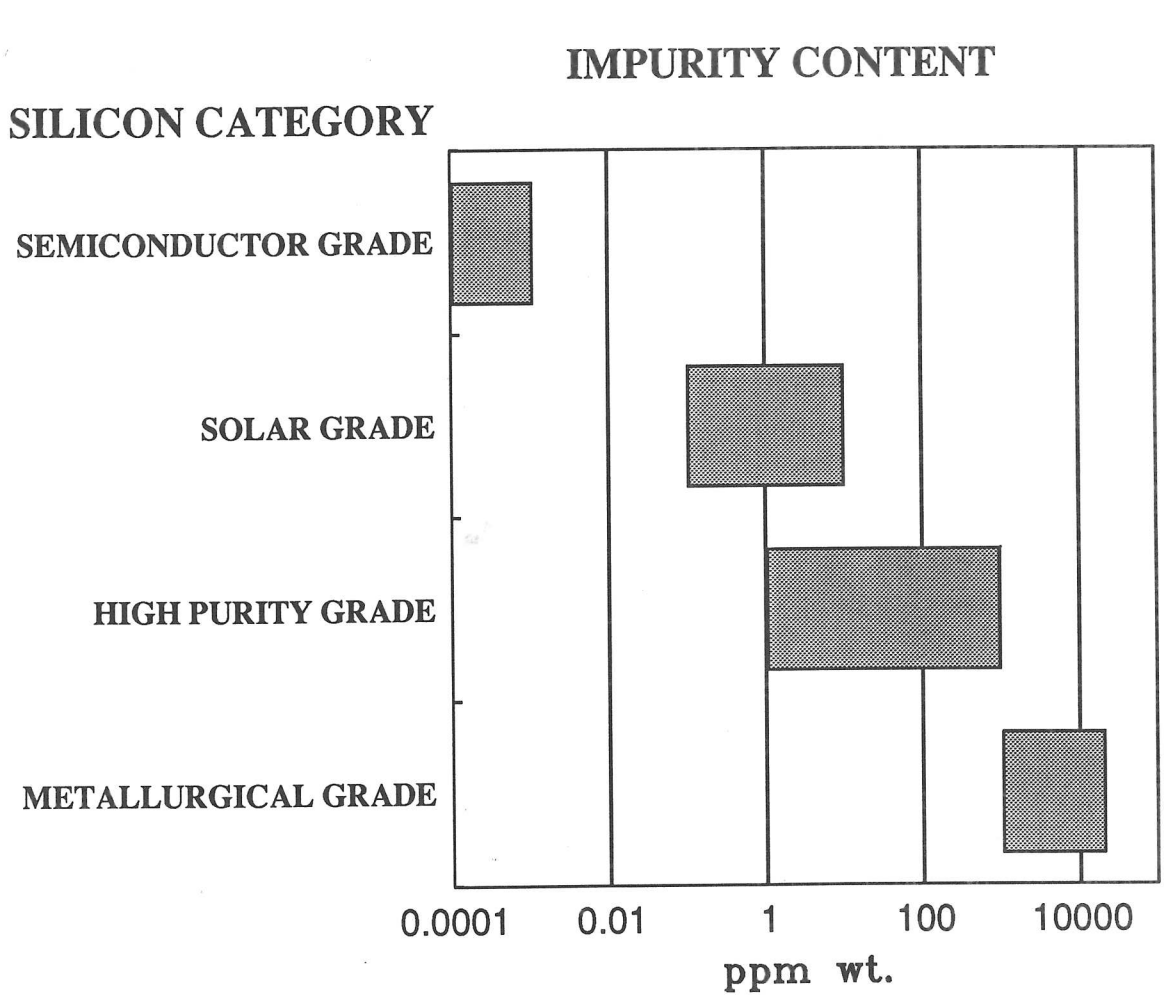

Figure 1 : Various grades of silicon metal [1].

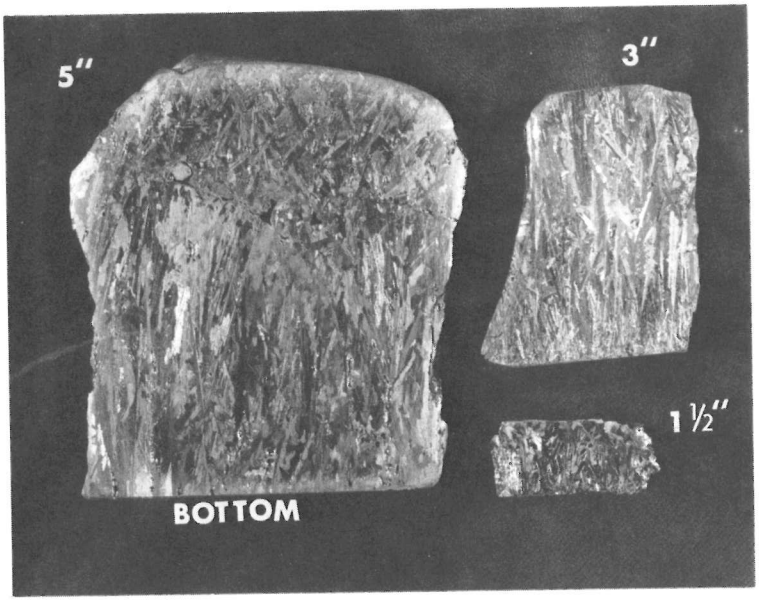

Figure 2 : Comparison of macrostructure of different thickness cast silicon metal specimens.

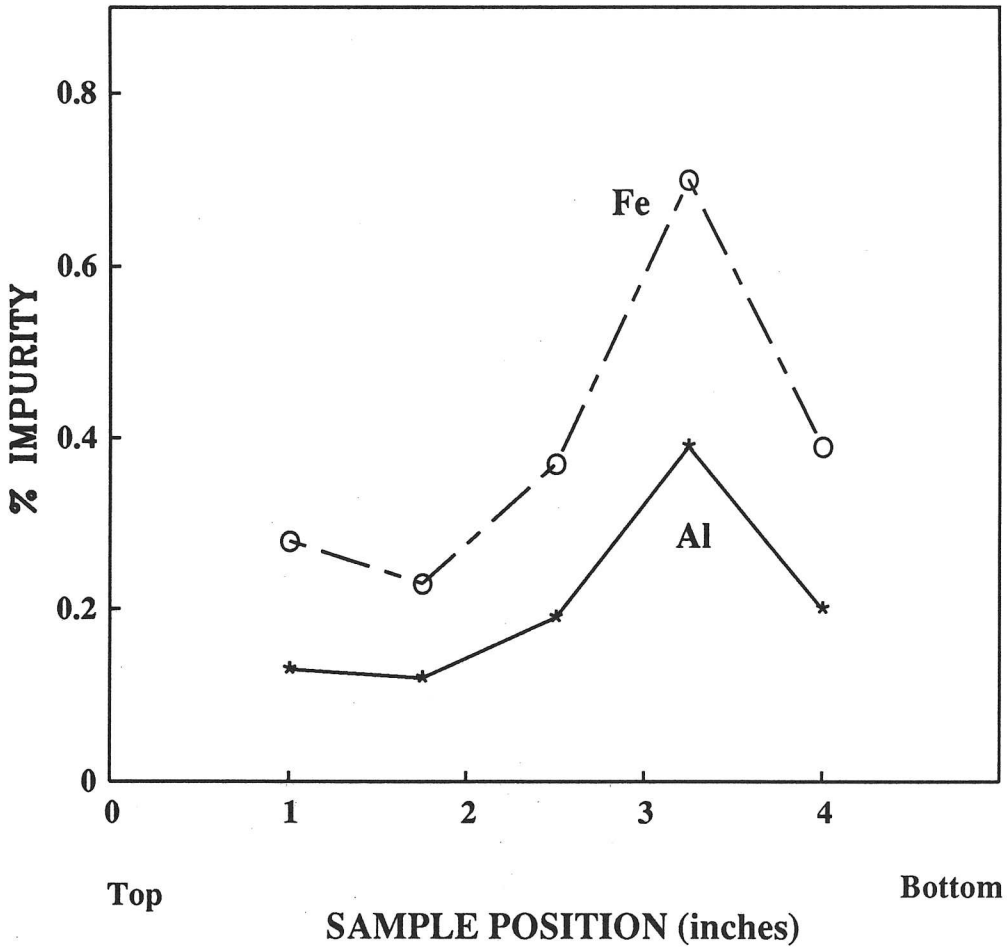

Figure 3 : Segregation of Fe and Al impurities along the height of a silicon metal casting.

(a) Segregated Zone

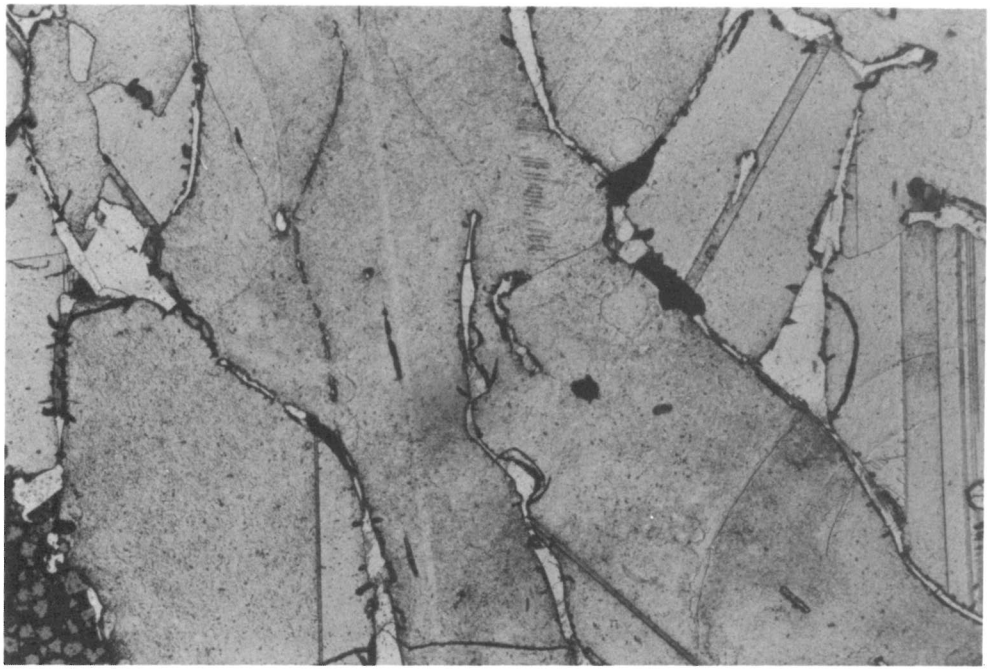

(b) Typical microstructure

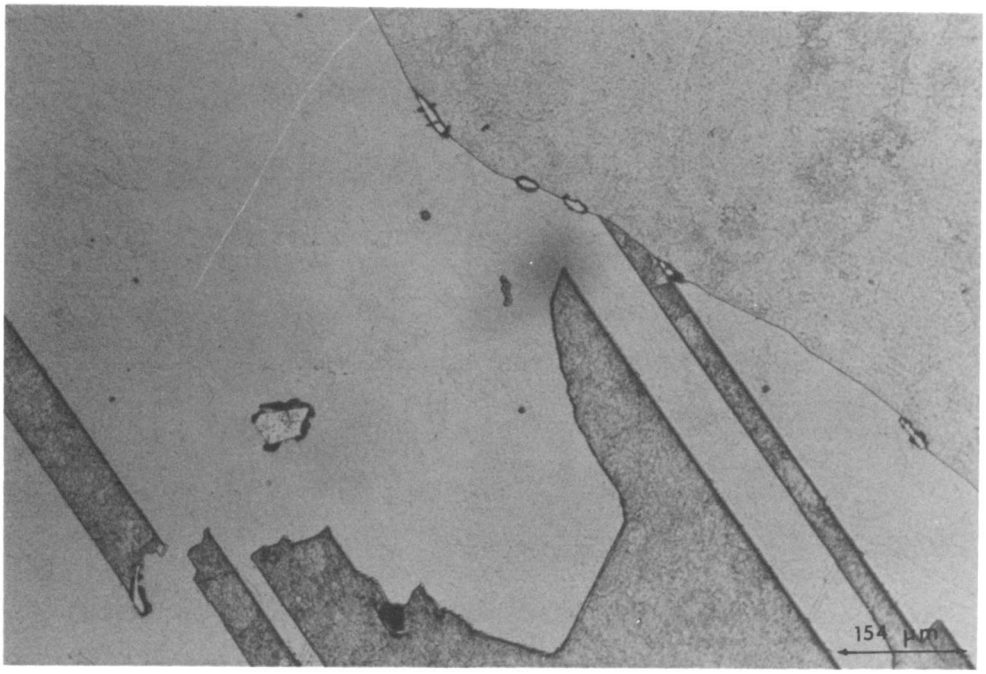

130X

Figure 4 : Microstructure of metallurgical grade silicon casting.

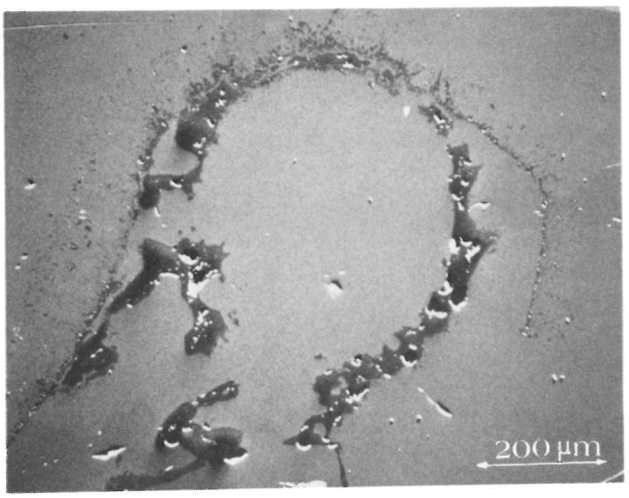

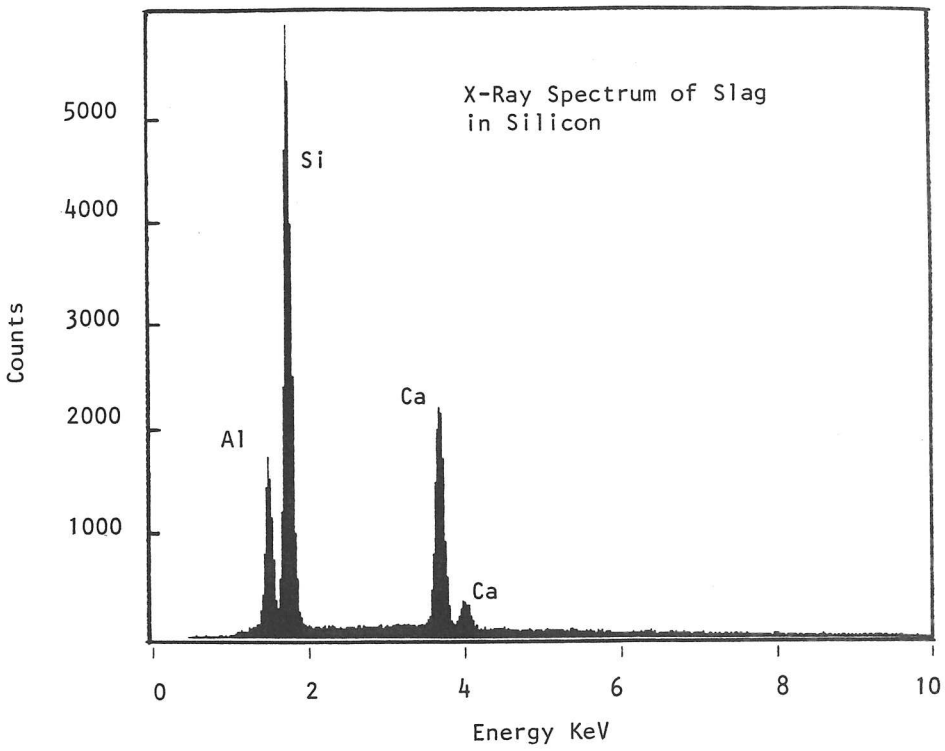

Figure 5 : A typical slag inclusion in silicon metal.

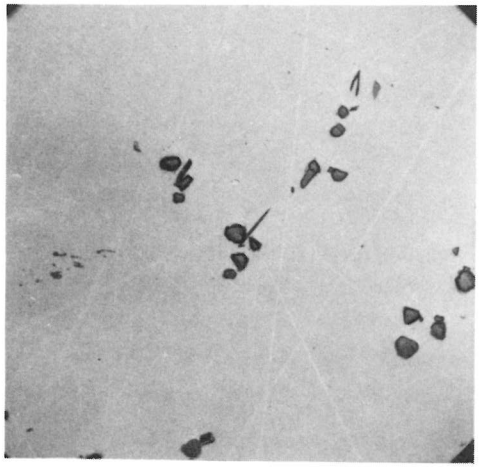

(a) Ordinary Reflected Light

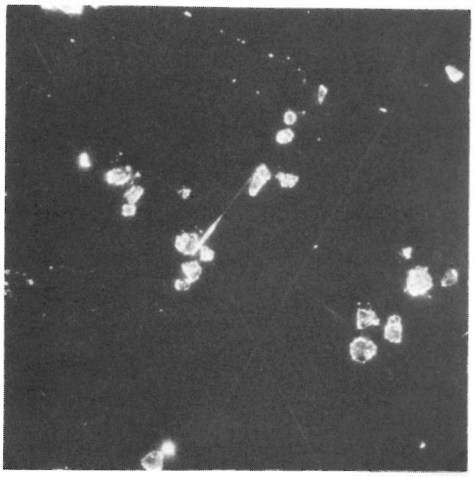

(b) Polarized Reflected Light

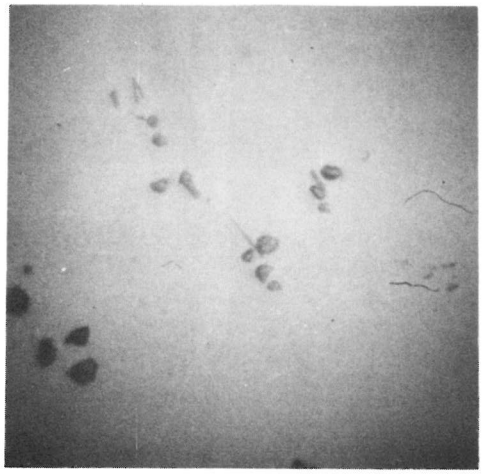

(c) Reflected Infrared Radiation

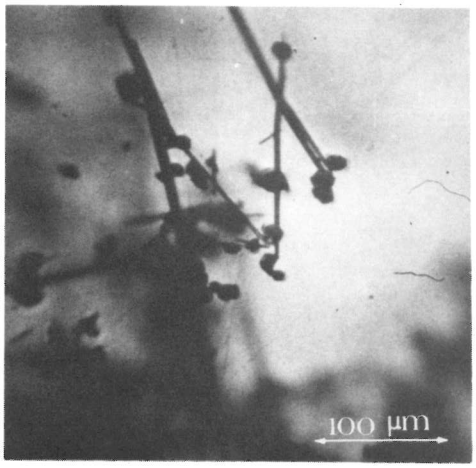

(d) Transmitted Infrared Radiation

200X

Figure 6 : Comparison of microstructure of silicon metal using various lighting methods.

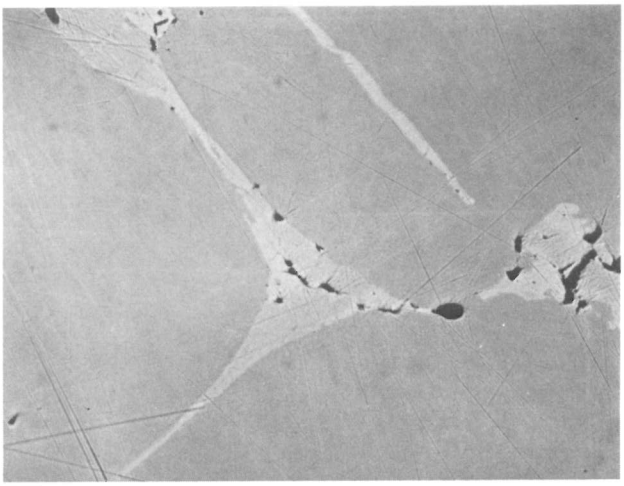

(a) Optical Image

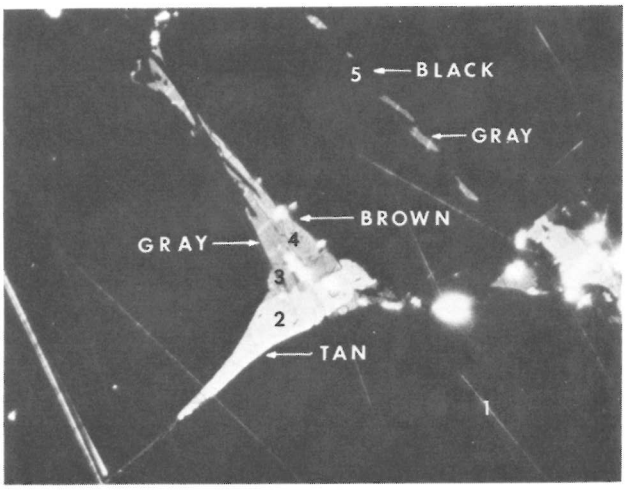

(b) Optical Image - Polarized Light

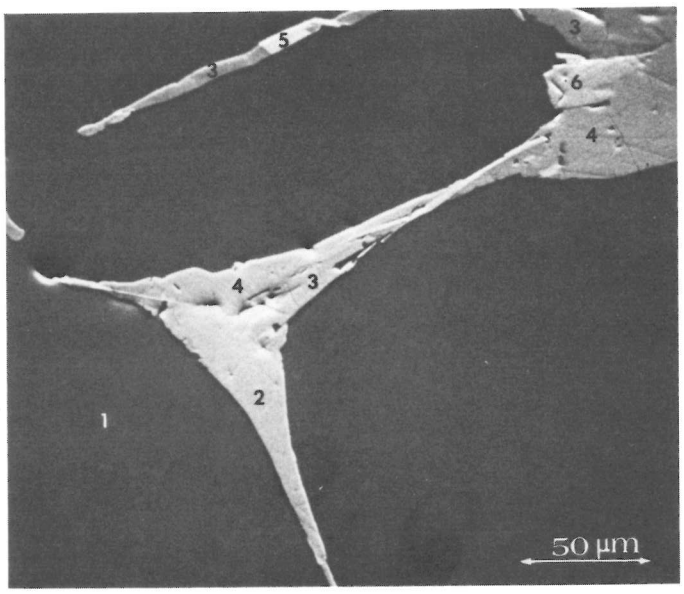

(c) SEM Image

400X

Figure 7 : Intermetallic phases in Al rich metallurgical grade silicon.

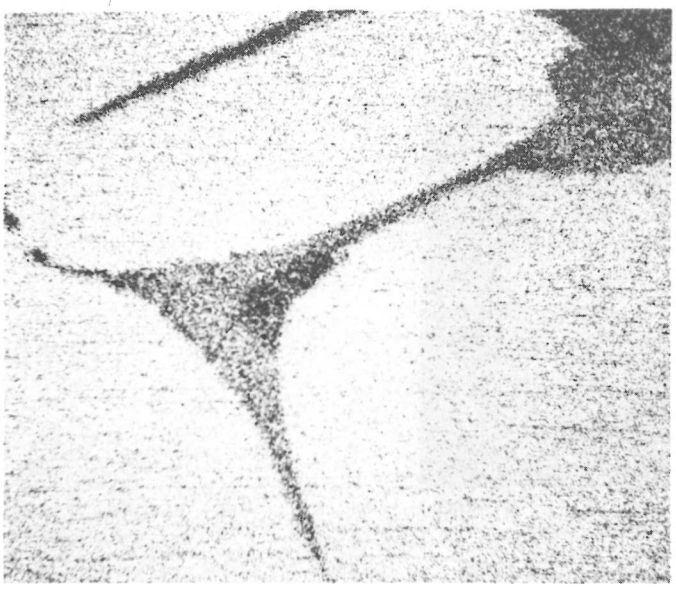

(d) X-ray Image - Si

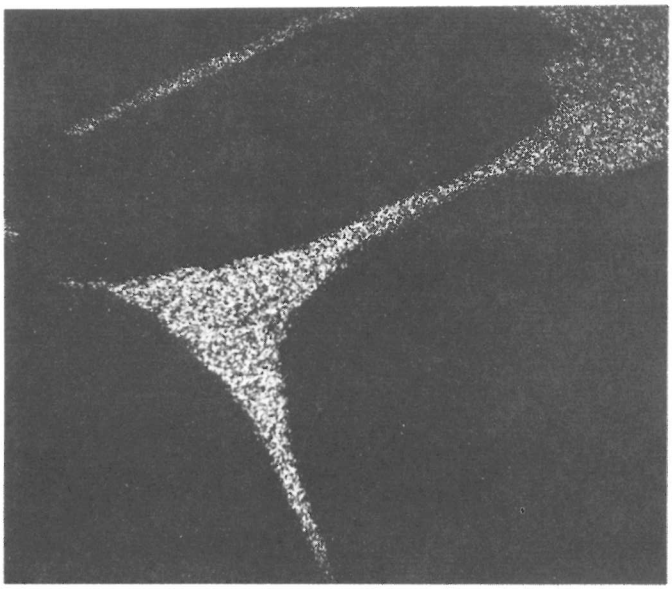

(e) X-ray Image - Fe

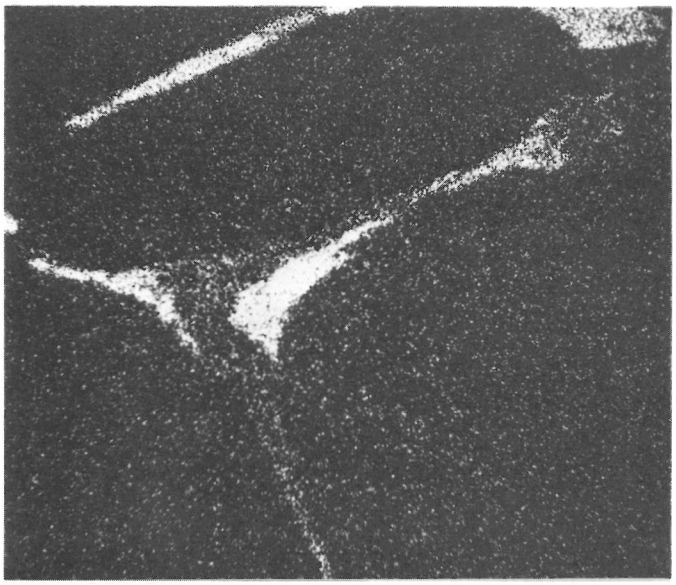

(f) X-ray Image - Al

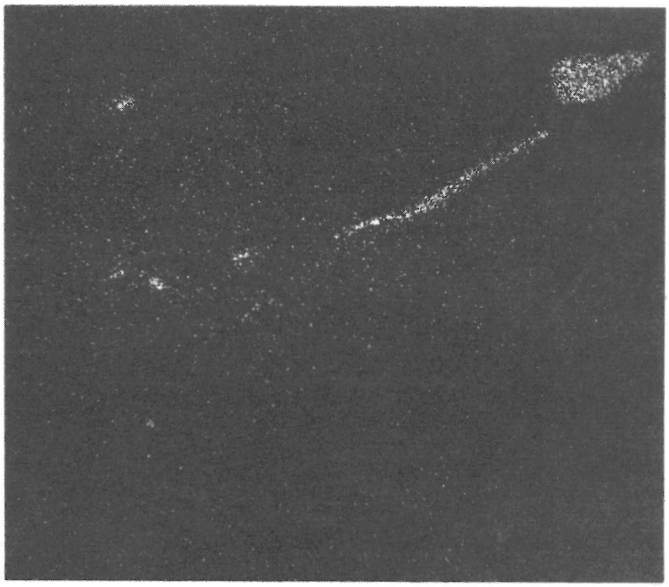

(g) X-ray Image - Ti

400X

Figure 7 : ..continued

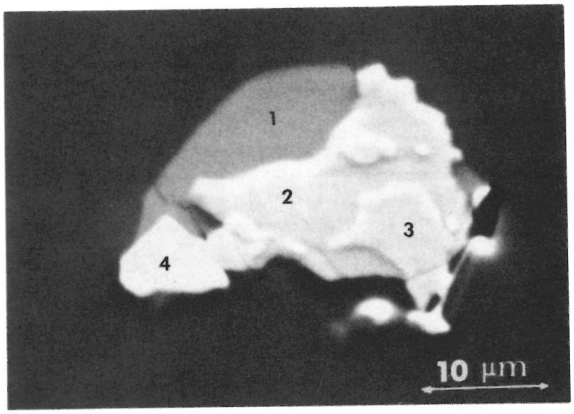

(a) SEM Image 2000X

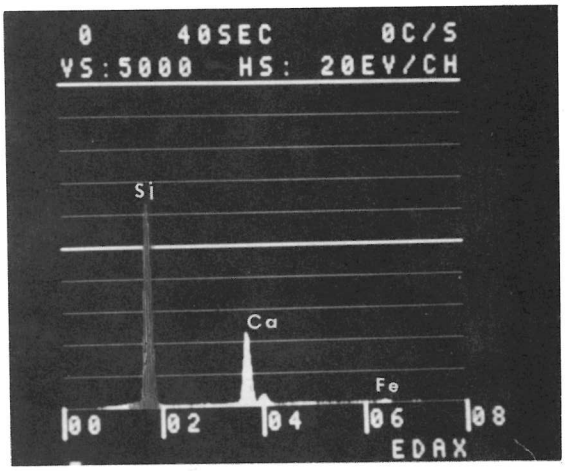

(b) Spot 1, X-ray Spectra

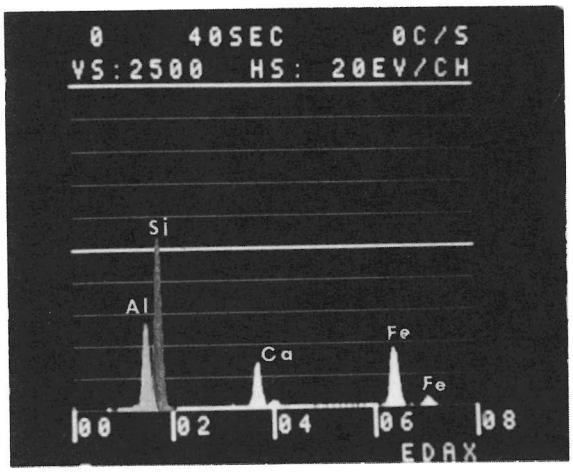

(c) Spot 2, X-ray Spectra

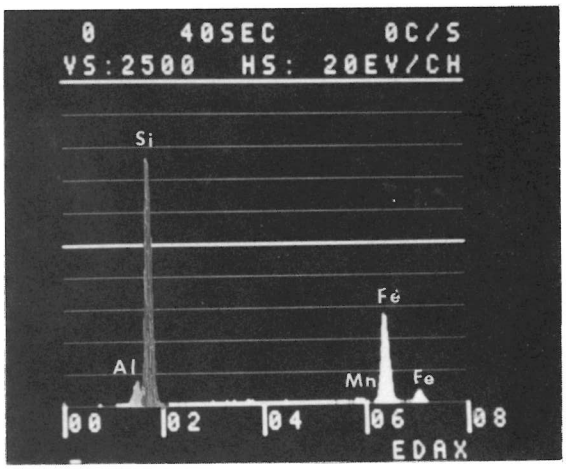

(d) Spot 3, X-ray Spectra

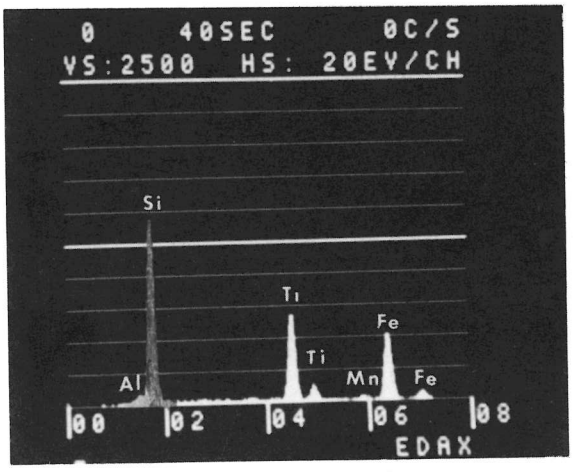

(e) Spot 4, X-ray Spectra

Figure 8 : Silicide phases in a metallurgical grade silicon

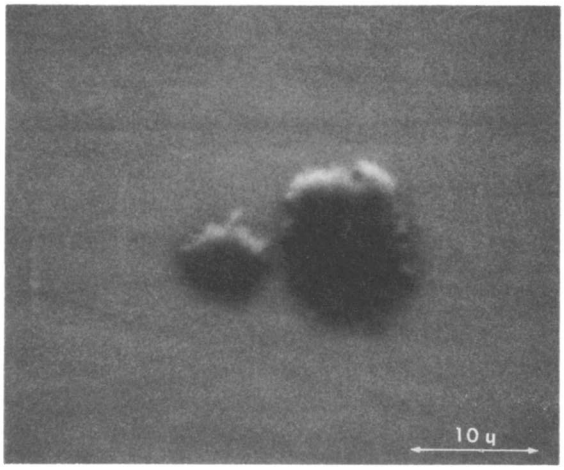

(a) SEM Image 2000X

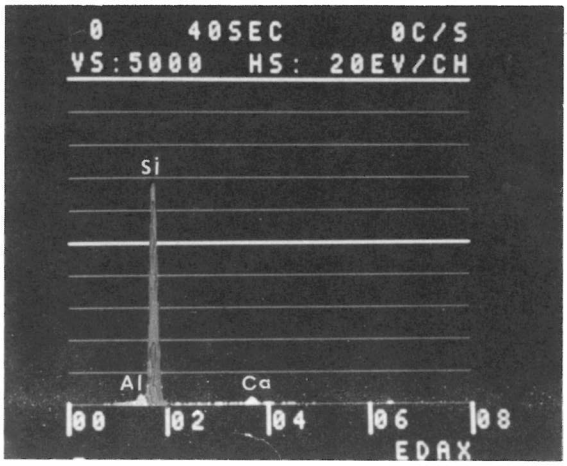

(b) X-ray Spectra

Figure 9 : A silicon carbide particle in a silicon matrix

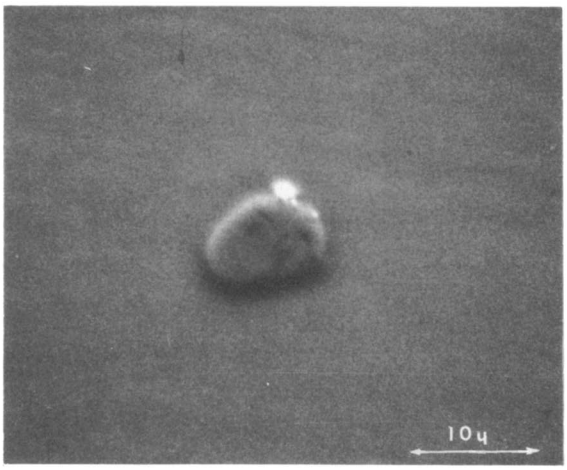

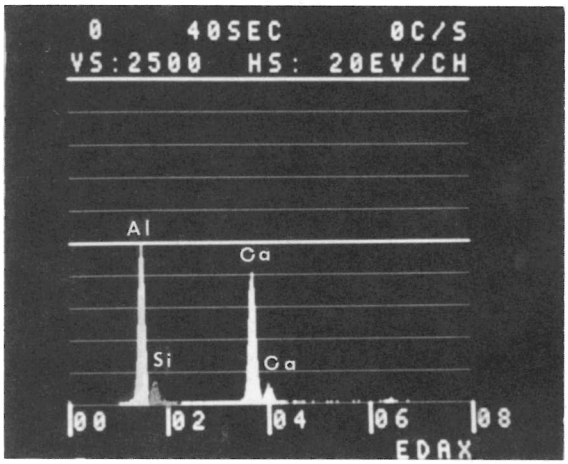

Figure 10 : A calcium aluminate inclusion in silicon matrix

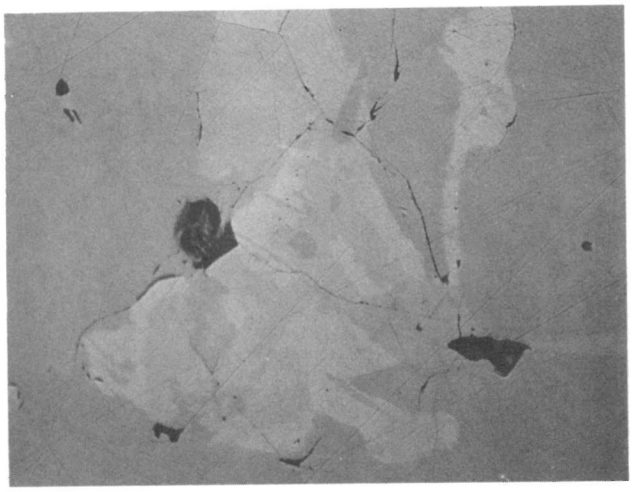

(a) Optical Image, 400X

(b) SEM Image, 200X

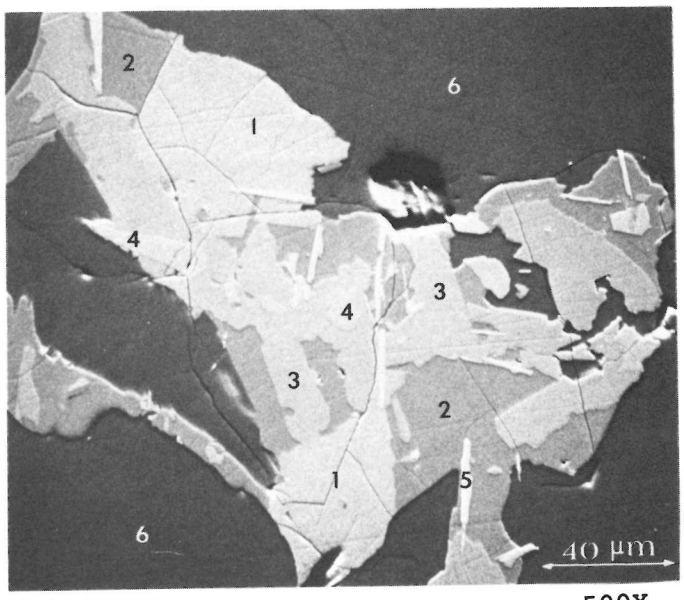

(c) SEM Image, 500X

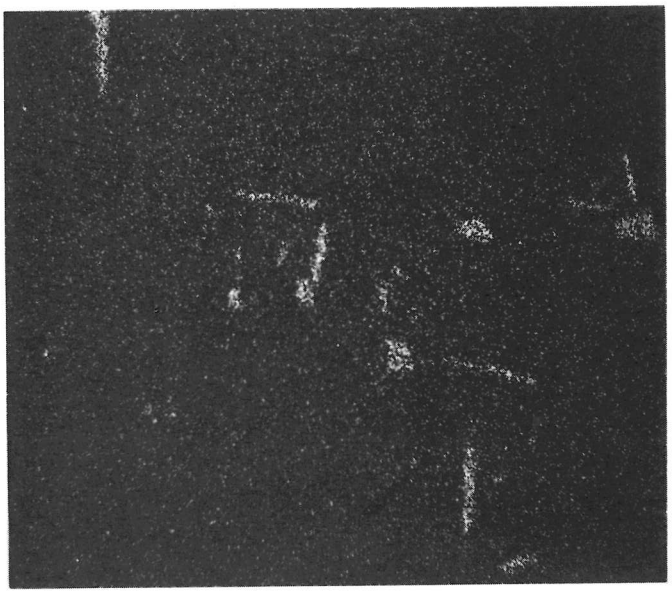

(d) X-ray Image - Ti

Figure 11 : Characterization of Intermetallic Phases in Silicon.

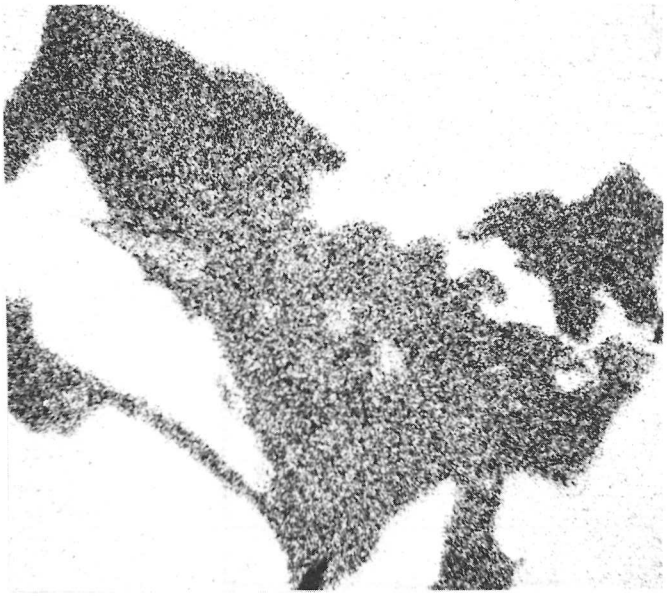

(e) X-ray Image - Si

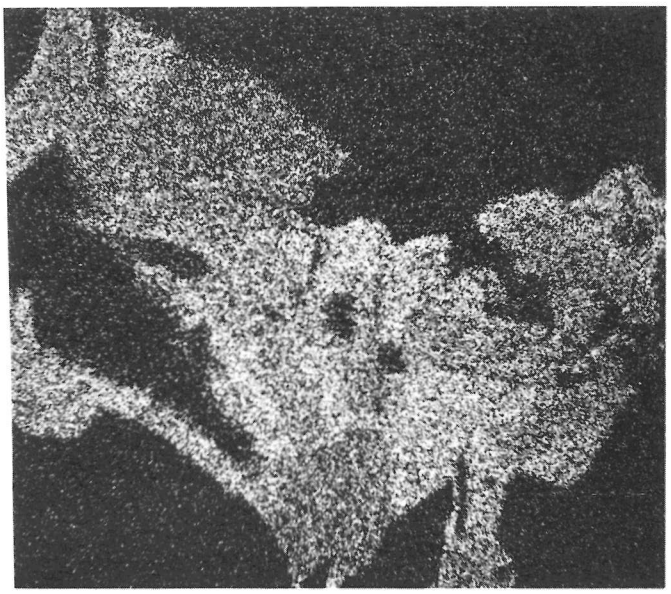

(f) X-ray Image - Al

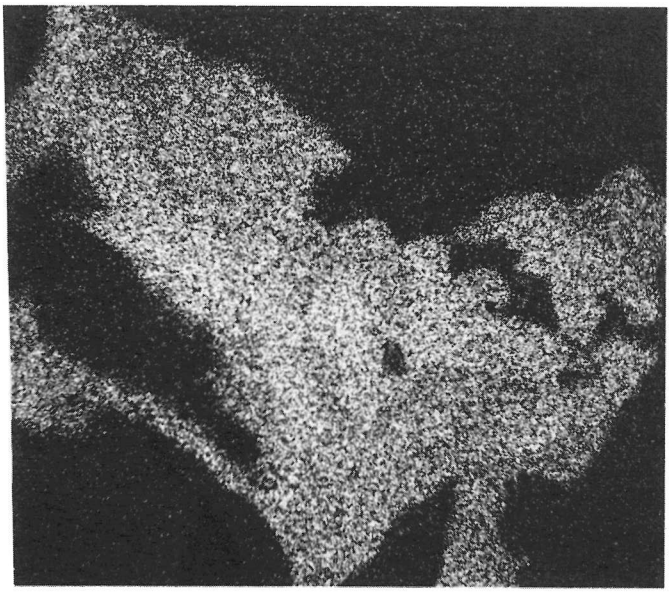

(g) X-ray Image - Fe

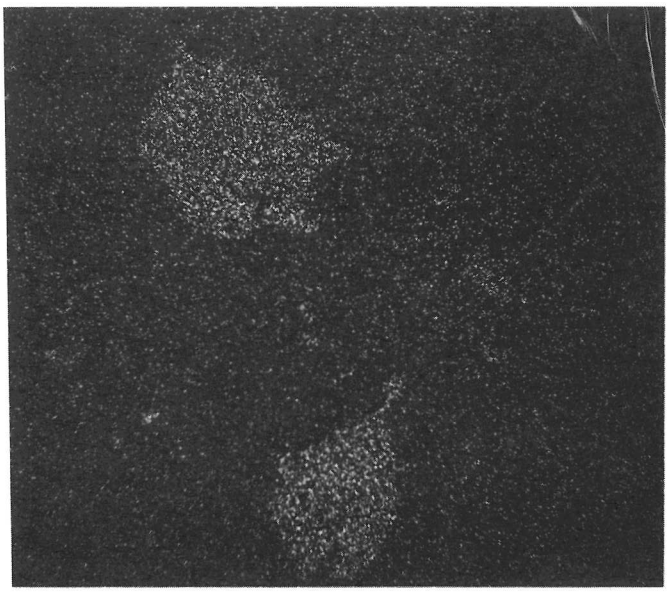

(h) X-ray Image - Ca

Figure 11 : ..continued

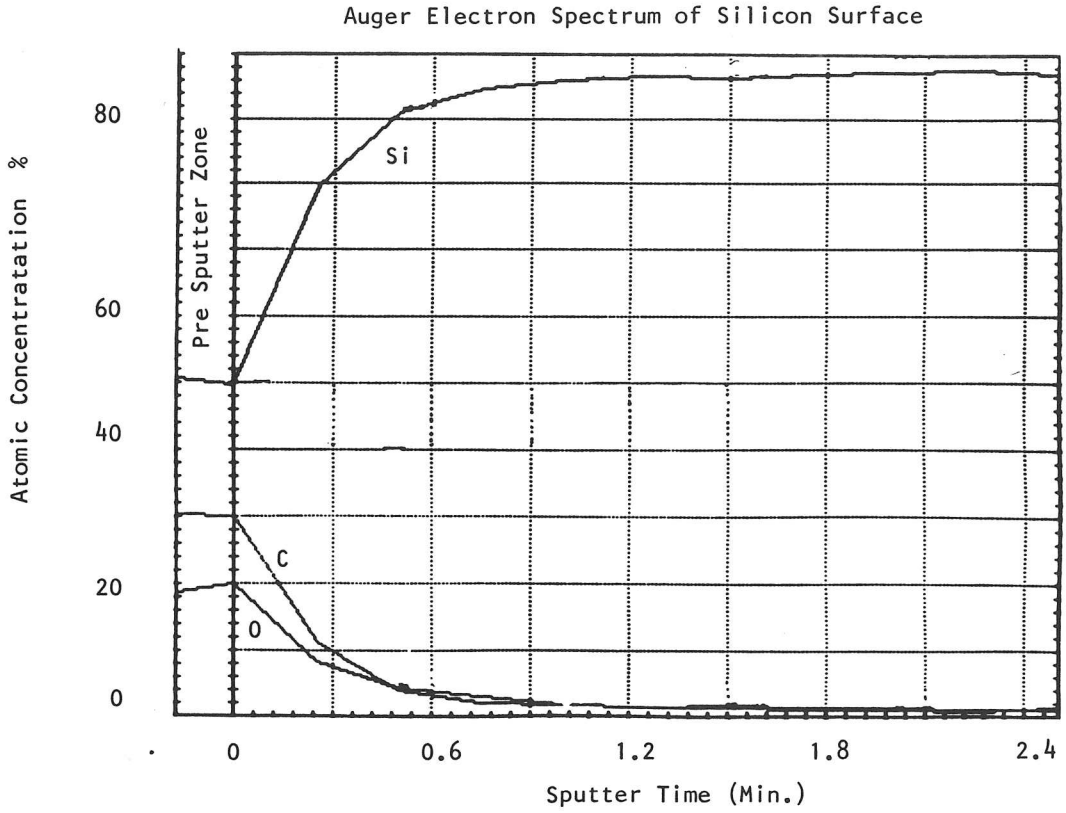

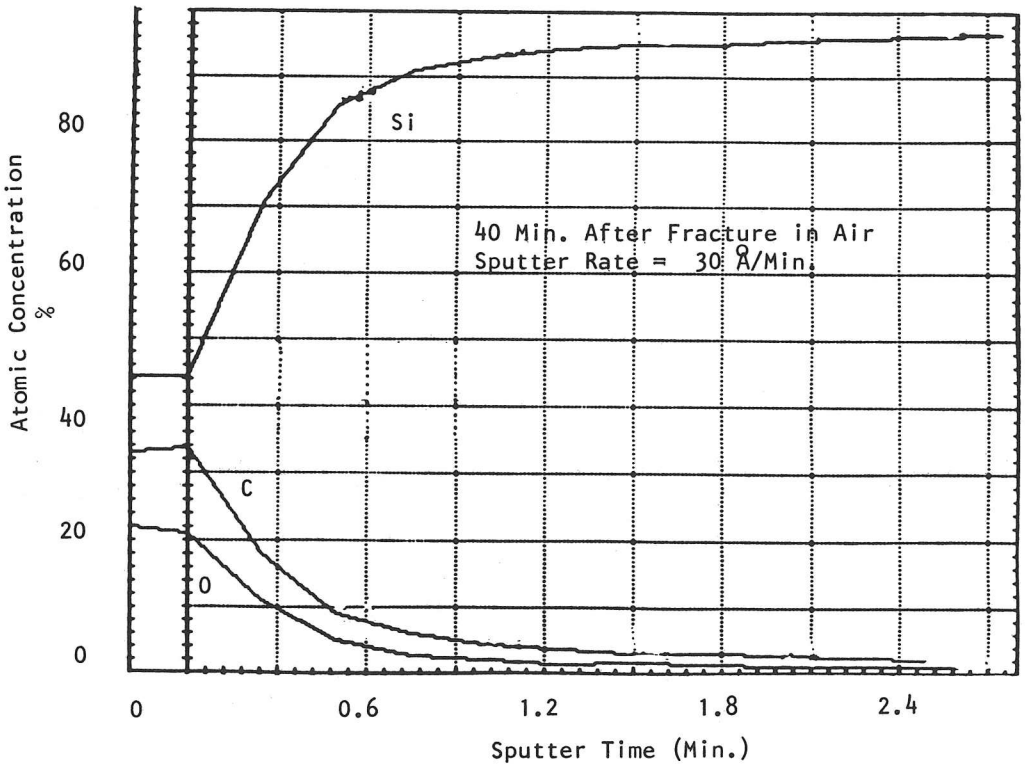

Figure 12 : Auger Electron Spectrum (AES) Concentration Profile for Si, O, and C obtained by ion milling a fracture surface.

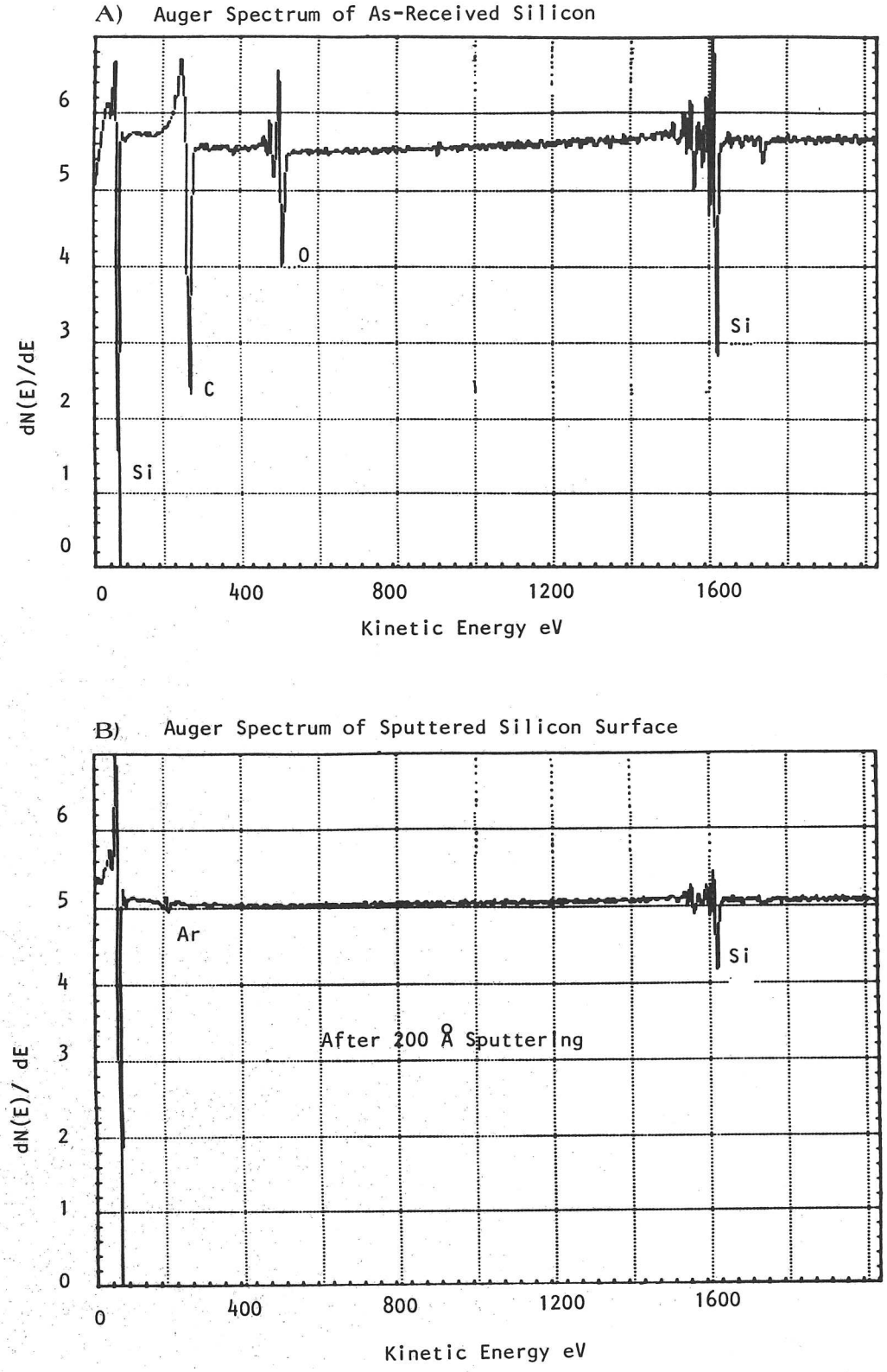

Figure 13 : Auger spectrum of Silicon surface

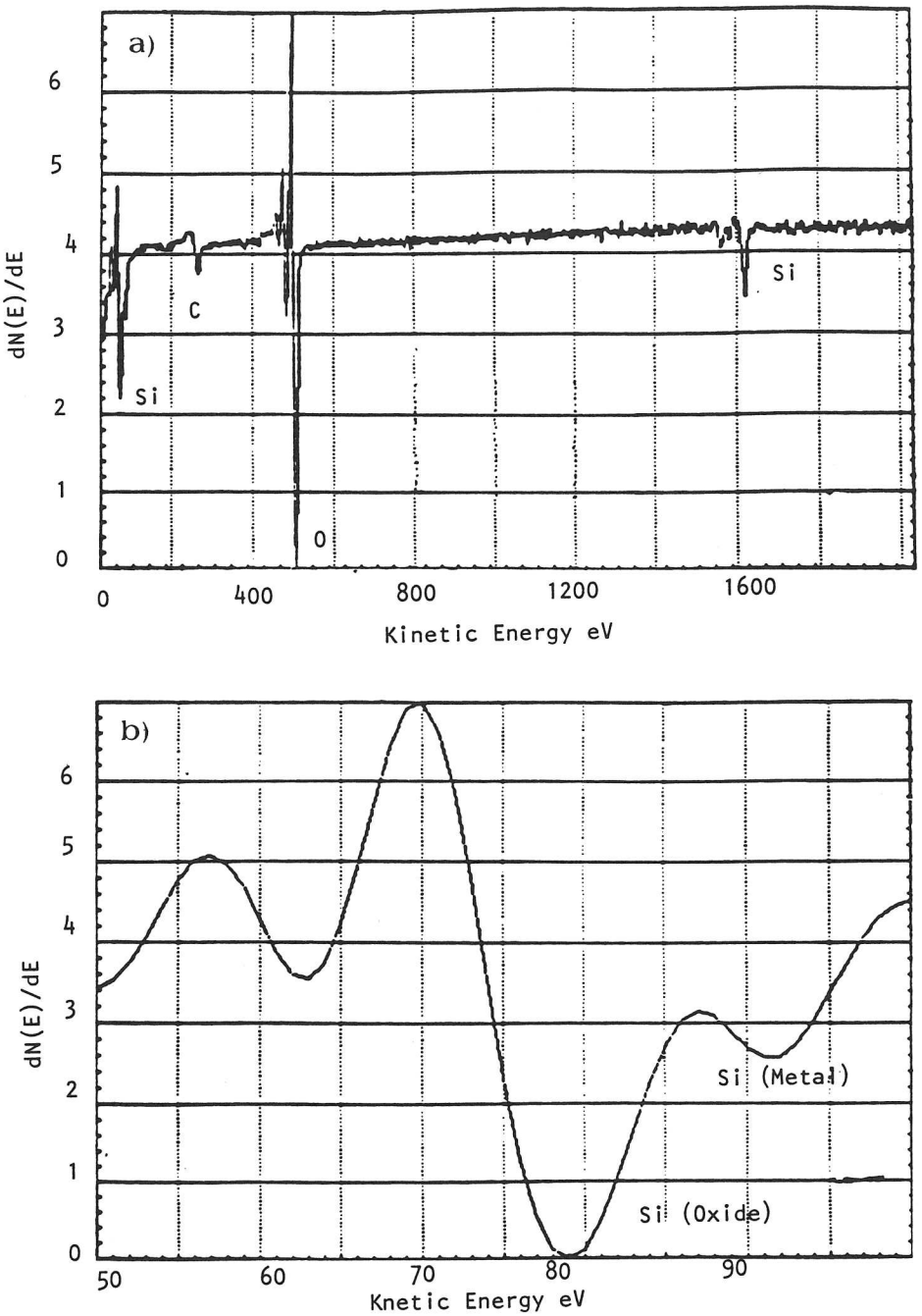

Figure 14 : Auger spectrum of a typical as-received siligrain particle surface.
(a) Spectrum range of 0 to 2000 eV
(b) Spectrum range of 50 to 100 eV

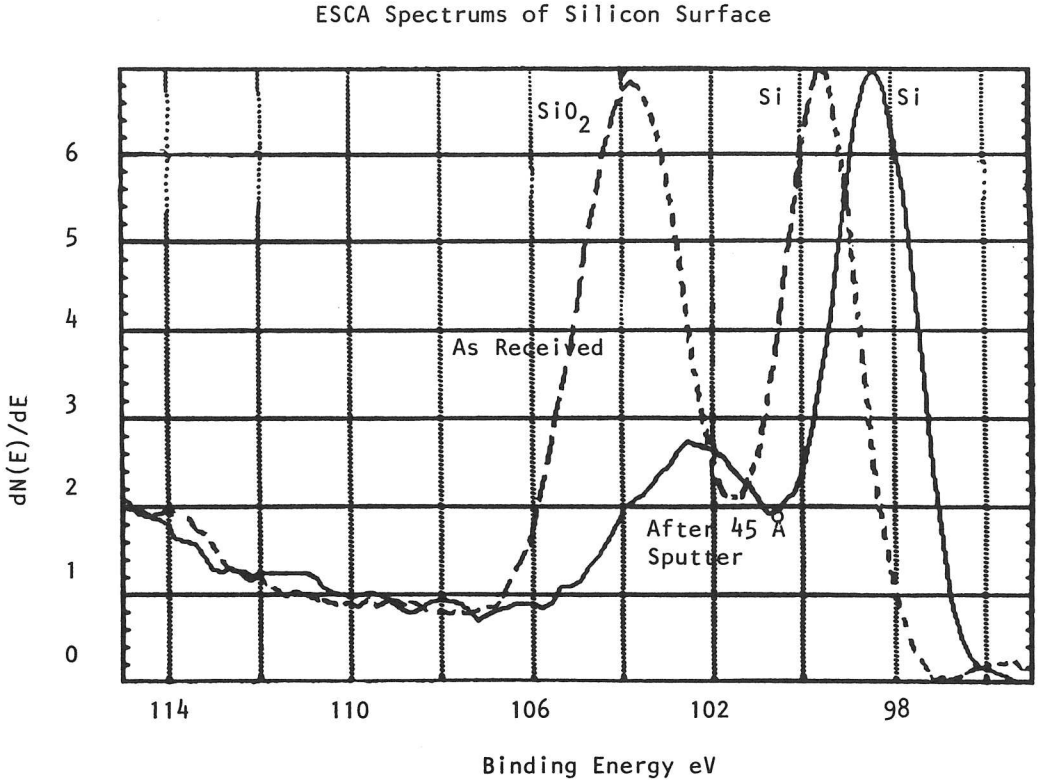

Figure 15 : Electron Spectroscopy for Chemical Analysis (ESCA) Spectra of silicon sample as-received and after sputtering a 45 A layer.

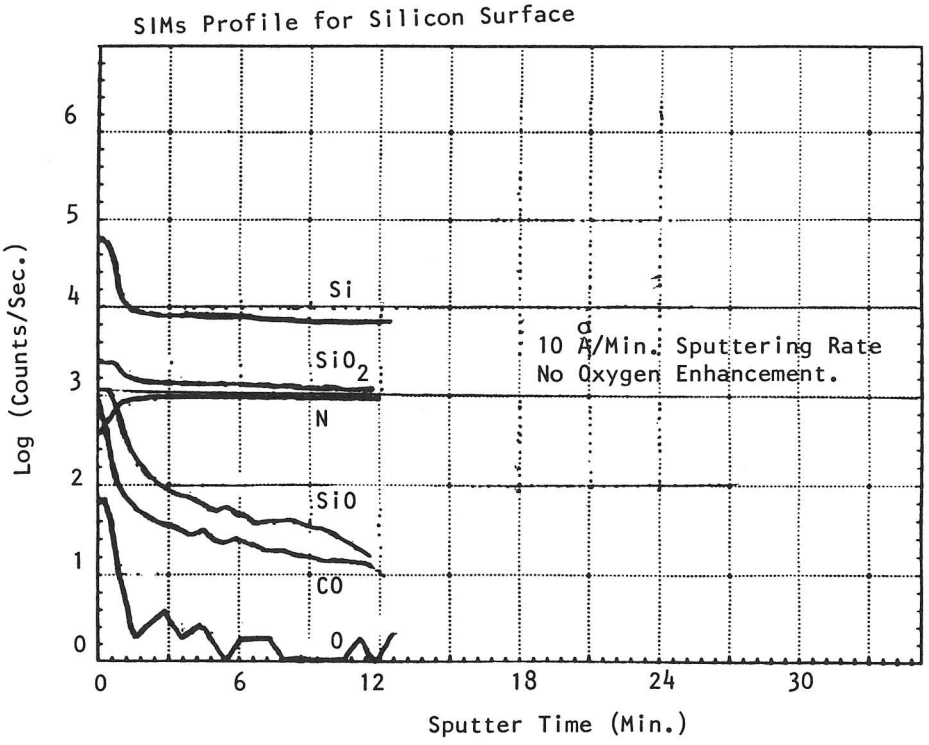

Figure 16 : Secondary Ion Mass Spectroscopy (SIMS) analysis showing the concentration profile of elements and possible compounds.